Journal of Applied Polymer Science

Predicting the Electrospinnability of Polymer Solutions with Electromechanical Simulation

Jonas Sidaravicius,[1,2] Ringaudas Rinkūnas,[1] Justinas Jurksus,[1] Tadeus Lozovski,[1,3] Isto Heiskanen,[4] Kaj Backfolk[4,5]

[1]Department of Solid State Electronics, Vilnius University, Sauletekio av. 9, Vilnius LT 10222, Lithuania
[2]Department of Polygraphic Machines, Vilnius Gediminas Technical University, J. Basanavicius street 28, Vilnius LT 03224, Lithuania
[3]University of Bialystok Vilnius Branch, Kalvariju street 143, Vilnius LT 03202, Lithuania
[4]Stora Enso Oyj, Imatra Research Center, FI 55800 Imatra, Finland
[5]Laboratory of Fiber and Paper Technology, Lappeenranta University of Technology, FI 53851 Lappeenranta, Finland
Correspondence to: J. Sidaravicius (E-mail: jonas.sidaravicius@ff.vu.lt)

The number of polymers successfully electrospun is increasing, and methods are needed predict the electrospinnability of polymers. With such methods, researchers should consider the polymer solution parameters and perform measurements in conditions that mimic the electrospinning process. A novel test method based on the electromechanical simulation of the fiber formation was developed. We formed fibers by mechanically dragging a conductive ball from the solution at an applied voltage and measuring the electrical current. The changes in the time of the electrical current (the ball current) reflect the fiber-formation process, which depended on certain polymer solution properties (e.g., viscosity, surface tension, liquid flow) and on the influence of charges on the fiber surface. The data obtained with the proposed method was compared with experimental data from electrospinning trials with the spinneret and bubble electrospinning. The results demonstrate that the ball-current method made it possible to predict the polymer solution behavior in the electrospinning process. © 2014 Wiley Periodicals, Inc. J. Appl. Polym. Sci. **2014**, *131*, 41091.

KEYWORDS: electrospinning; fibers; properties and characterization; theory and modeling

Received 2 May 2014; accepted 3 June 2014
DOI: 10.1002/app.41091

INTRODUCTION

Electrospinning is a simple, versatile, and cost-efficient technique for producing nanofibers with fiber diameters in the range of a few nanometers to a few micrometers.

Many polymers have been tested in the electrospinning process.[1–18] For example, Huang et al.[3] reported in 2003 that more than 50 polymers had been successfully electrospun. Apparently, the number of electrospinnable polymers is significantly higher today as the research and applications of nanotechnology and other technologies is increasing rapidly. Nanoelectronics,[3,4,6,9,19] core–shell fibers,[20] and the engineering of biodegradable polymers are examples of emerging applications that use electrospinning technology,[5,6,9]

One of the challenges of electrospinning is the production of nanofibers of high and uniform quality at a high intensity or high production rate. The range of polymers electrospinnable from an aqueous system is still relatively limited. This is partly due to the lack of information concerning the connection between the material properties and Taylor cone formation and the subsequent deposition of nanofibers and the process intensity. The electrospinning process is affected by a large number of parameters and process variables, and their influence on the process is still not fully understood, especially not for multiple-nozzle or large-scale deposition systems. Consequently, each new polymer solvent system requires a long and tedious trial-and-error procedure in a laboratory environment, and this may not be industrially applicable or upscalable.

Many researchers have attempted to find relationships between the polymer solution properties, process variables, and electrospinnability with regard to the fiber quality (thickness, absence of beads, etc.) and process intensity. It is well known that the electrospinning process depends on parameters such as the viscosity, surface tension, solution concentration, polymer molecular weight, viscoelasticity, solvent, electrical conductivity, and dielectric properties of the solution. Important process variables include the solution feed rate, the electric potential geometry of the electric field, the distance between the spinneret and the

ground electrode, the temperature, and the relative humidity. The ability of the polymer solution to be electrospun in a particular case is determined by most of the parameters mentioned together, although their roles are not equal.

The viscosity of the polymer solution is one of the most important parameters for the electrospinning process. Fong et al.[21] investigated the electrospinning of poly(ethylene oxide) (PEO) ethanol-to-water solutions and found that a viscosity in the range of 1–20 poise and a surface tension between 35 and 55 dyne/cm were suitable for fiber formation. At viscosities above 20 poise, electrospinning was impossible because of the instability of flow due to the high cohesiveness of the solution. Droplets were formed instead of fibers when the viscosity was too low (<1 poise). In ref. 22, the electrospinning of cellulose acetate was investigated, and it was claimed that a viscosity between 1.2 and 10.2 poise was suitable for fiber formation. These examples clearly demonstrated that the viscosity ranges of different polymer solutions that are electrospinnable are essentially different. The solvent affects the electrospinnability viscosity range. Cellulose acetate was electrospun in a mixture of acetone and dimethylacetamide, but it could not be electrospun successfully in these solvents individually.

Another parameter that greatly influences the electrospinning process is the surface tension. The surface tension of the solution determines at least partly the electrical field threshold required to initiate Taylor cone formation and subsequent electrospinning. The surface tension influences the fiber morphology, and when the surface tension of the polymer solution is reduced, fibers can be obtained without bead formation. This is, however, a complex process, and it is limited to certain systems. The surface tension effect is probably a function of solvent–polymer interaction and the compositions, and therefore, a reduction in the surface tension will not always promote the electrospinning. For example, in acetone (23.7 dyne/cm), cellulose acetate showed short fibers and beads on a string, whereas in dimethylacetamide (32.4 dyne/cm), it showed only beads, and in the mixture, fibers free of beads were obtained.[22] So, this investigation and many others proved that the surface tension of the solution together with its viscosity cannot be the controlling parameter, and it impossible to assert that these are viscosity and surface tension values above or below which the polymer is no longer spinnable. This statement was confirmed by our own experiments (unpublished) with sodium carboxymethylcellulose in water, for which the viscosity and surface tension were the same as that of PEO dissolved in water. The latter solution showed very good spinnability, whereas the sodium carboxymethylcellulose did not electrospin at all.

Koski et al.[23] investigated the electrospinning of poly(vinyl alcohol) (PVA), and they found that fiber formation essentially depended on the polymer concentration and molecular weight. To explain their results, Koski et al. used a model proposed by Hong et al.[24] based on the metric $[\eta]C$, where $[\eta]$ is the intrinsic viscosity and C is the concentration. This metric characterizes the intermolecular interaction, which is important for fiber formation. Polymer chain entanglement is needed, and it was found that at $[\eta]C > 4$ (the semidilute entangled regime), fibrous structures were obtained. So, this metric may be the parameter needed to predict the electrospinnability. There is, however, no evidence that such an approach confirms such a prediction and that the criterion $[\eta]C > 4$–5 can be successfully applied to predict the electrospinnability of other polymers.

In many studies,[25–30] a method of predicting the electrospinnability and estimating the nanofiber diameter and quality based on the De Gennes scaling concept[31] has been used. According to this concept, a double-logarithmic plot against C of the specific viscosity $\eta_{sp} = (\eta_s - \eta_0)/\eta_0$, where η_s and η_0 are the zero-shear viscosities of the solution and solvent, respectively, contains several regions with different slopes. As the concentration passes from the semidilute unentangled area (with $\eta_{sp} \approx C^{1,25}$) to the semidilute entangled area (with $\eta_{sp} \approx C^{4,8}$), a change in slope is observed when the concentration exceeds the entanglement concentration (C_e). It was found that in many cases, C_e is the minimum concentration for the formation of fibers. Vetcher et al.[25] tested several polyacrylamides (PAAs) and found that at a low molecular weight, PAA formed only globular products, and no fiber formation was observed. This was explained by the fact that all of the concentrations of these polymers were below C_e. PAA with a weight-average molecular weight (M_w) above 80,000 g/mol produced mostly beads when $C < C_e$ and fibers when $C > C_e$; this was in good agreement with data obtained with other polymers. However, the statement of Vetcher et al. was not quite correct. For example, McKee et al.[26] found that although neutral polymer solutions produced electrospun fibers with beads at C_e, a salt-free poly(dimethylaminoethyl methacrylate) solution did not form fibers at concentrations less than $8C_e$ and that the addition of NaCl (up to 50 wt %) lowered the minimum concentration for fiber formation to $1.5C_e$. Therefore, the prediction of electrospinnability based on the rheological properties of the polymer solution is a useful but not universal method. In addition to molecular entanglement, other aspects of intermolecular interaction must be taken into account.

To predict the transfer from electrospraying (beads) to electrospinning (fibers), Shenoy et al.[32] defined the solution entanglement number $[(n_e)_{soln}]$ as the ratio of M_w of the polymer to the entanglement molecular weight in solution. Fiber formation is initiated at $(n_e)_{soln} \approx 2$ (or when the number of entanglements per chain ≈ 1) or higher. This approach provides an *a priori* prediction of polymer concentration for electrospinnability without the need to measure the solution viscosities. This approach is, however, valid only for a good solvent where polymer–polymer interactions are negligible. In ref. 32, it was also noted that other important factors, such as solvent quality (polymer solubility in the solvent), must be taken into account. Therefore, as with the C_e criterion, the metric entanglement number is not universal, and in many cases, the determination of the entanglement molecular weight is not simple.

In a number of publications, efforts have been described to find the controlling parameter discussed previously, below which the polymer is no longer spinnable, or merely to determine whether a particular polymer solution is electrospinnable at all. In addition to the parameters already mentioned, the solvent dielectric permittivity or polarizability,[33] the solution electroconductivity,[34]

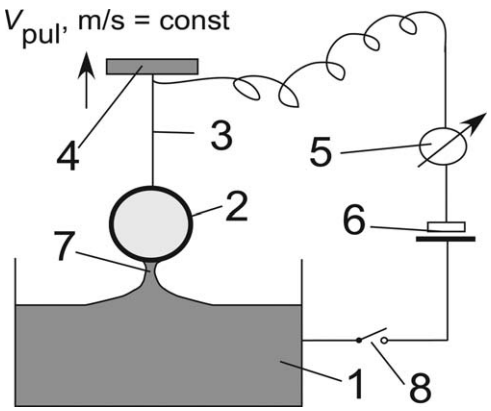

Figure 1. Schematic picture of the ball method: (1) polymer solution, (2) metallic ball, (3) conductive wire connected to the ball and pulling mechanism, (4) pulling mechanism, (5) ammeter, (6) direct-current source (low voltage), (7) solution fiber, and (8) switch. V_{pul}, ball pulling velocity, m/s.

some jet formation features (e.g., the length of the linear part, the geometry of the fiber coils),[35] and together, the solution electrical conductivity, surface tension, viscosity, and so on[36] have been studied.

So the fundamental task remains, that is, to find a reliable method for predicting whether it is possible to electrospin the polymer in a particular solution. Such a method is necessary because the field of nanofiber applications is expanding, and more and more new electrospinnable polymers of different classes are needed. The ability of a polymer to electrospin is usually determined by the testing of a polymer solution in a real process and the changing of the solution formulation and electrospinning parameters. This trial-and-error procedure is not simple and requires advanced electrospinning equipment.

A fundamental understanding of Taylor cone formation and its role in electrospinning is still lacking, and current methods of predicting the ability or efficiency to electrospin a polymer in a particular solution are not complete and lack the conditions needed to imitate an electrospinning process.

In this study, we describe a method that was developed to simulate the electrospinning process. In this method, one forms a fiber by pulling mechanically a ball from the polymer solution under an applied voltage. The applied voltage induces charges on the surface of the immersed ball, and an electrical current passes through the fiber; this makes possible a precise electrical monitoring of the fiber formation. Fiber formation in such a process depends on all of the solution properties (the viscosity, surface tension, electrical conductivity, liquid flow, etc.) and on the charges created on the wet fiber surface. The data obtained with this electromechanical simulation have been compared with the electrospinning process to develop an understanding of the predictability of the electrospinnability of polymer solutions.

EXPERIMENTAL

Materials

Several aqueous polymer solutions were tested. The polymers used were PEO (Sigma-Aldrich, four grades with M_w values of 600,000, 900,000, 2,000,000, and 4,000,000 g/mol), PVA [partly hydrolyzed (88%), Mowiol 10–88, Kuraray], carboxymethylcellulose (CMC; FinnFix 150, CP Kelco), and ethylhydroxyethylcellulose (EHEC; Bermocol, Akzo Nobel). All solutions were prepared by the dissolution of the polymer in distilled water under stirring at an elevated temperature (up to 90°C). The electromechanical simulation of the electrospinning process was performed with the setup shown in Figure 1, and the electrical current (ball current) was monitored.

Method

We evaluated Taylor cone and fiber formation and the extensional properties of the solution by pulling fluid from the surface of a polymer solution at constant speed. A ball (2) was fixed with a thin electroconducting wire (3) on the lifting mechanism (4; Figure 1). The polymer solution (1) was poured into a small vessel. A voltage was then applied to the ball from the battery (6) through the lifting mechanism and wire, and the other pole of the battery was connected with the solution. The circuit included an ammeter (5) and a switch (8). By lifting the ball and simultaneously measuring the current through the elongated polymer solution in the interface, we analyzed the fiber formation kinetics.

The test was performed with the ball immersed in the polymer solution. When the direct-current source was switched on, the electrical current was measured and recorded. The ball was lifted at a constant velocity, and the electrical current was measured.

Initially, the current was constant (Figure 2), and its value depended on the conductivity of the polymer solution. When the ball was lifted, a fiber was formed, and the current decreased because of the fiber became longer and thinner. The fiber finally broke, and the current dropped to zero. Thus, the formation of the fiber was monitored precisely through the measurement of the electrical current, as shown in Figure 1. The typical current kinetics are shown in Figure 2. For convenience, the electrical current value was normalized by the

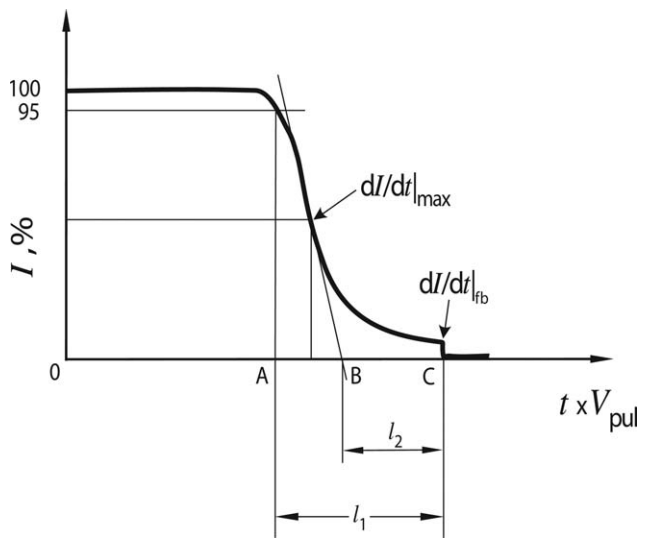

Figure 2. Electrical current kinetics during the pulling of the ball from the fluid. *I*, electrical current; *t*, time.

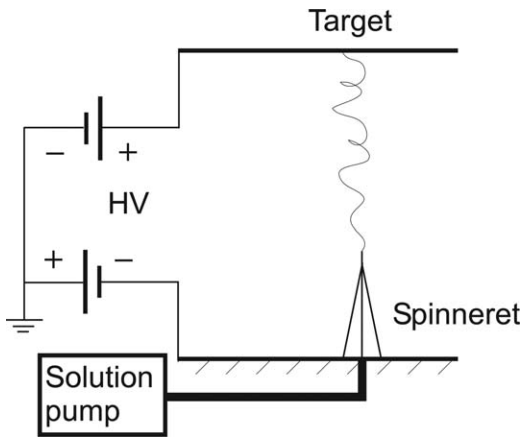

Figure 3. Electrospinning spinneret setup. HV, high voltage source.

division of the current value by maximum value and is expressed in percentages. From this curve, the final length before the break of the formed fiber and several parameters that describe the electrical current kinetics curve could be determined. The fiber length (l_1; Figure 2) was calculated as the product of the time at which the ball fully left the fluid to fiber break and the ball lifting velocity. This length was an indication of the polymer's ability to form jets and polymer fibers. If this length was small, spinning was impossible, and only electrospraying could be expected. If the length was large, electrospinning was possible.

Because the determination of the point when ball left the fluid was difficult, it was reasonable to take the point at which the current was 95% of its initial value. The fiber break point was the time when the electric current dropped to zero.

Because of the viscoelastic properties of the polymer solutions, the stretching of the fiber was not a linear process. At least two processes governed the fiber formation: fluid pulling out and fiber thinning. In the first stage, fluid pulling out was dominant, and in the final stage, fiber thinning dominated. So it was reasonable to assume that thinning began at the inflection point where the current change velocity was at maximum (dI/dt_{max}). The current change velocity at fiber break (dI/dt_{fb}) and the length of the thinning stage (l_2) were also determined, as shown in Figure 2.

The fiber formation depended on the ball dimensions and ball lifting velocity. Balls of different dimensions were tested, from 10 μm (the end of a wire) to 15 mm. The most reliable results were obtained with a 9-mm ball.

l_1 depended on the ball lifting velocity. At a very low velocity, gravity forces strongly influenced the process, and the lifting velocity had to be high but not too high. At very high velocities, the viscoelastic properties of the solution were suppressed, and the fiber formation strongly differed from the fiber formation in electrospinning. A velocity of 40 mm/s gave the most reliable results.

Electrospinnability Assessment

The electrospinnability was assessed with two methods: spinneret electrospinning and electrospinning from a foamed surface. The spinneret electrospinning apparatus consisted of a syringe with a needle (inner diameter = 1.5 mm), solution pump, target, and two high-voltage (30-kV) sources connected to the target and the needle (Figure 3). The distance between the needle and target was 20 cm.

Electrospinning from the foamed surface was performed with the setup shown in Figure 4. Compressed air was fed into a tube equipped with holes, which then created bubbles and foam (7) from which electrospinning occurred. The nanofibers were deposited on a metal or glass.

The deposited coatings were then studied with atomic force microscopy (AFM; Nanomics MultiView 1000; intermittent scanning mode, 256 × 256 resolution, tip diameter = 20 nm) and an optical microscope.

RESULTS AND DISCUSSION

More than 20 different polymer solutions were tested with the proposed method, and the deposited nanofibers were further analyzed with AFM or optical imagery. Three types of deposition were distinguished: (1) individual drops, (2) drops and nanofibers with beads, and (3) nanofibers without beads. Case 1 occurred only in electrospraying, whereas case 3 was observed when the polymer was electrospun. Case 2 was an intermediate between electrospraying and electrospinning. Typical ball-current kinetics are shown in Figure 5 and Figures 7 and 9 (shown later) together with AFM or optical images. The ball-current kinetics showed different slopes and breaking lengths. PEO (M_w = 900,000 g/mol) at a low concentration (Figure 6) showed a sharp drop in the current, and l_1 and l_2 were very short (2 and 0.07 mm, respectively); this showed that the associative interactions (entanglement) within the polymer chains were too weak to form a fiber.[31] Therefore, we expected that this solution could not be electrospun and that only electrospraying would take place. Electrospinning tests with both methods showed that the deposited material formed droplets rather than fibers (Figure 6).

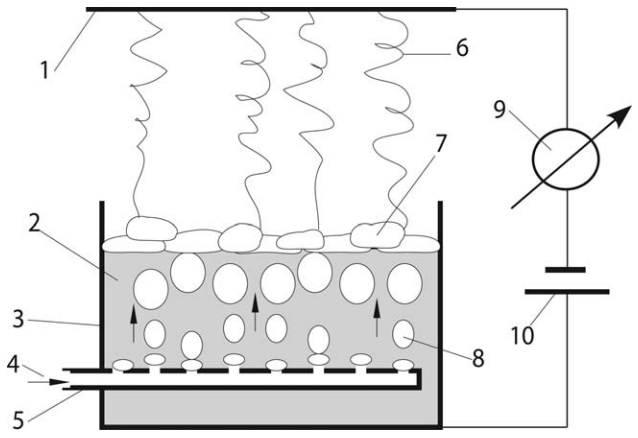

Figure 4. Electrospinning apparatus: (1) collector, (2) polymer solution, (3) vessel on the electrode, (4) compressed air, (5) tube with holes, (6) nanofibers, (7) foam bubbles, (8) bubbles in the solution, (9) ammeter, and (10) high-voltage source (60 kV).

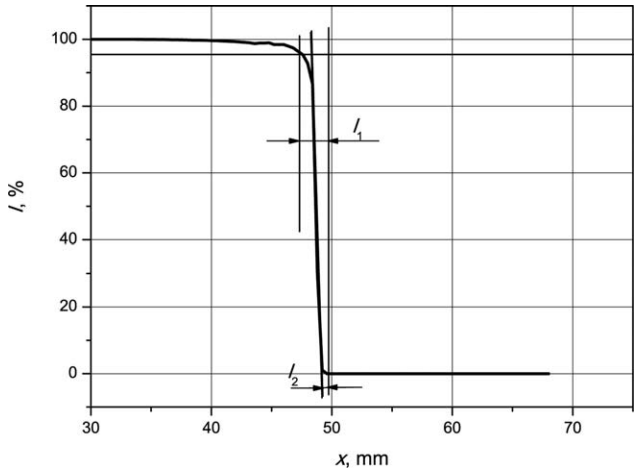

Figure 5. Ball-current kinetics of a 10 mg/mL PEO solution ($M_w = 900{,}000$ g/mol). I, electrical current normalized to 100%; l_1, fiber length; l_2, length of the fiber thinning stage; x, ball pulling distance.

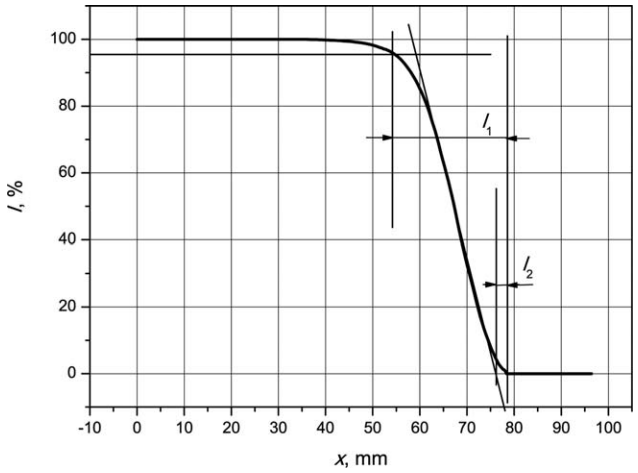

Figure 7. Ball-current kinetics determined for PEO at a concentration of 50 mg/mL ($M_w = 900{,}000$ g/mol). I, electrical current normalized to 100%; l_1, fiber length; l_2, length of the fiber thinning stage; x, ball pulling distance.

When the polymer concentration was increased, the ball-current kinetics changed significantly (Figure 7). The fiber was longer with $l_1 = 23.2$ mm and $l_2 = 3.5$ mm. This means that the associative interaction within the polymer molecules was much stronger and sufficient for the formation a Taylor cone and subsequently a nanofiber. The photomicrograph (Figure 8) of the deposited samples shows that nanofibers and drops were deposited.

Figure 9 shows the ball-current kinetics of the PVA (Mowiol 10–88; $C = 130$ mg/mL). l_1 was slightly longer, and l_2 was much longer. This indicated a strong interaction between molecules and suggested that good electrospinning could be expected. The AFM scan (Figure 10) showed that such a prediction was correct.

These data and figures indicate that there was a correlation between the electrospinnability and the ball-current kinetics parameters, and this was confirmed by all of the experiments in this study. Table I presents all of the data obtained with the ball-current kinetic parameters and the electrospinnability in 22 experiments with different polymers at different solution concentrations. The data are divided into three groups on the basis of the morphological structure of the depositions: electrospraying, electrospraying with electrospinning (drops and fibers with beads), and electrospinning. The analysis of the ball-current kinetics parameters showed that all four parameters could provide information for predicting the electrospinnability of the polymer solution. l_2 was more informative because the differences in this parameter in the three groups were evident. We could predict that when l_2 was between 0 and 0.5 mm, only electrospraying was possible; when it was between 0.5 and 2.0 mm, electrospraying together with the formation of fibers occurred, and when l_2 was over 8–10 mm, good electrospinning could be expected. The parameter l_2 was interlinked with the parameter dI/dt_{fb}, which also provided information for predicting the electrospinnability. At dI/dt_{fb} values of greater than 200%/s, only electrospraying was expected. At dI/dt_{fb} values

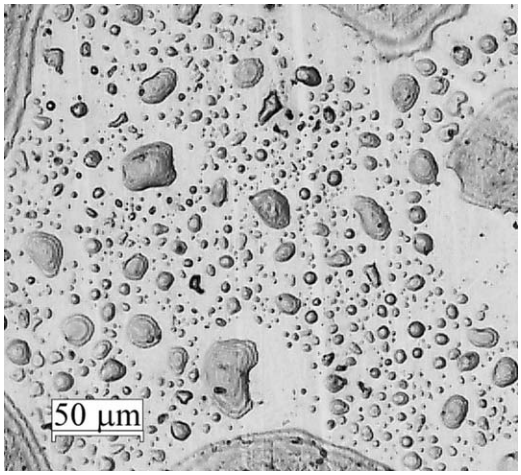

Figure 6. Photomicrograph of PEO deposited on a substrate ($M_w = 900{,}000$ g/mol, concentration = 10 mg/mL.).

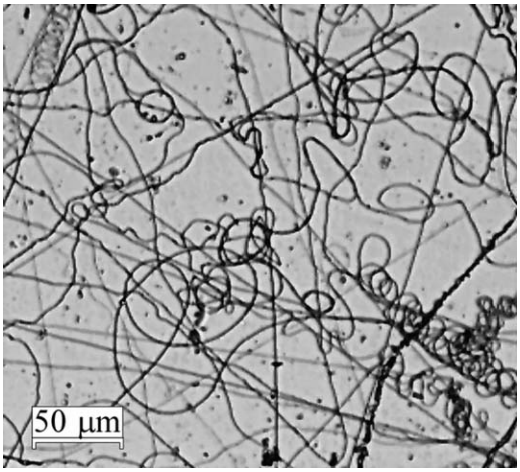

Figure 8. Photomicrograph of PEO deposited at a 50 mg/mL concentration ($M_w = 900{,}000$ g/mol).

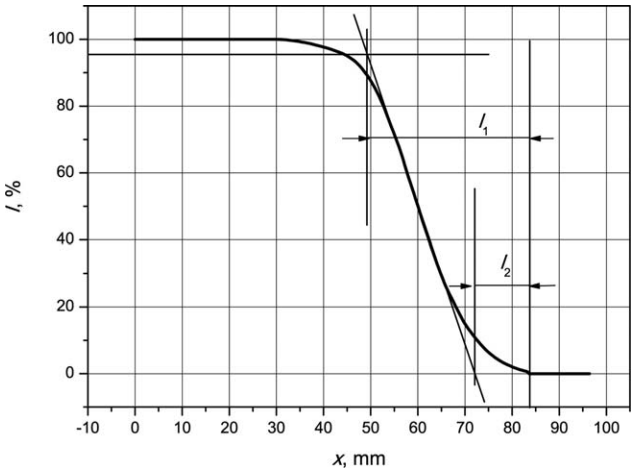

Figure 9. Ball-current kinetics for PVA at a concentration of 130 mg/mL (Mowiol 10–88). *I*, electrical current normalized to 100%; l_1, fiber length; l_2, length of the fiber thinning stage; *x*, ball pulling distance.

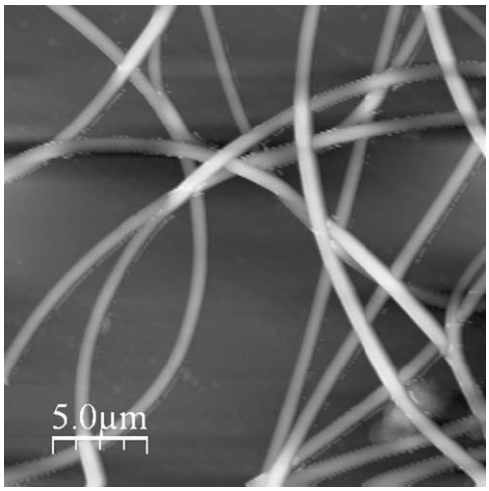

Figure 10. Topographic AFM image of the PVA fibers deposited at a concentration of 130 mg/mL (Mowiol 10–88).

Table I. Parameters of the Ball-Current Kinetics and Electrospinning Results

Polymer	Concentration (mg/g)	Solvent	l_2 (mm)	dl/dt_{fb} (%/s)	dl/dt_{max} (%/s)	l_1 (mm)	Electrospinning/ electrospraying
Electrospraying							
PVA 10-88	10	Water	0.07	4646	5954	2.0	Electrospraying
PVA 10-88	40	Water	0.23	2214	5812	2.4	Electrospraying
EHEC	10	Water	0.14	3300	3500	4.3	Electrospraying
EHEC	10	Water plus ethanol	0.42	1343	2036	4.7	Electrospraying
PEO (M_w = 900,000)	10	Water	0.44	482	622	2	Electrospraying
CMC		Water	0	9554	9554	0.8	Electrospraying
Water	—	—	0	8180	8180	1.2	Electrospraying
Electrospraying/electrospinning							
PVA 10-88	70	Water	0.55	322	2508	4.7	Electrospraying and traces of electrospinning
PVA 10-88	70	Water	0.61	171	2744	4.6	Electrospraying and traces of electrospinning
PEO (M_w = 600,000)	20	Water	0.99	268	2236	4.4	Electrospraying and traces of electrospinning
PVA 10-88	100	Water	1.72	104	925	9.7	Electrospinning with beads
PEO (M_w = 900,000)	20	Water	1.1	132	260	4	Electrospinning with beads
PEO (M_w = 900,000)	50	Water	3.5	44	267	23	Electrospinning with beads
PEO plus PVA	55	Water	1.54	100	807	10.31	Electrospinning with beads
PEO (M_w = 4,000, 000)	46	Water	1.62	58	363	20.5	Electrospinning with beads
PEO (M_w = 900,000)	40	Water	1.7	87	441	15.7	Electrospinning with beads
PEO (M_w = 4,000, 000)	40	Water	1.83	64	550	15.3	Electrospinning with beads
Electrospinning							
PVA 10-88	130	Water	12.4	13.6	183	39	Electrospinning
PEO (M_w = 600,000)	70	Water	15.3	12,3	117	55.3	Electrospinning
PEO (M_w = 900,000)	90	Water	24.5	9.4	95	73.5	Electrospinning
PEO (M_w = 900,000)	110	Water	11.7	17	125	54.3	Electrospinning
PEO (M_w = 2,000, 000)	70	Water	7.9	17	182	37.2	Electrospinning

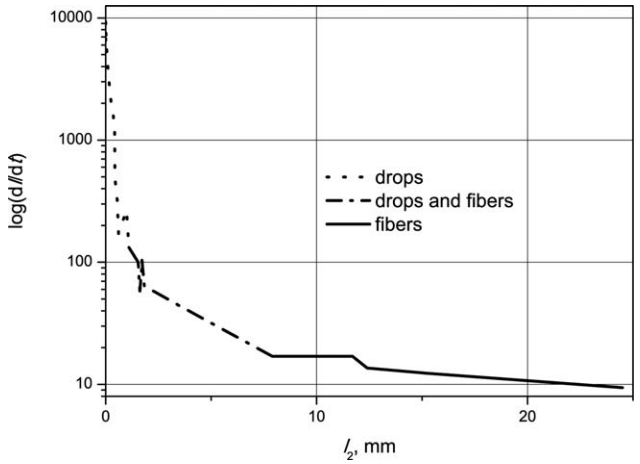

Figure 11. Interdependence of parameters l_2 (length of the fiber thinning stage) and electrical current I change rate dI/dt_{fb}.

between 200%/s and 10–20%/s, electrospraying together with the formation of fibers occurred, and at dI/dt_{fb} values of less than 10–20%/s, good electrospinning was possible. The relationship between the two parameters is evident in Figure 11. The solid line shows the range of electrospinning, the dash–dot range shows where fibers with beads were formed, and the dot region shows where electrospraying occurred. However, the boundary between electrospraying and electrospraying together with electrospinning was not as obvious as in the case of l_2. The parameters l_1 and dI/dt_{max} also provided information for predicting electrospinning, but it was more difficult to determine the ranges at which the different processes (electrospraying, electrospraying with electrospinning, or electrospinning) could be expected.

CONCLUSIONS

The test method developed showed that the Taylor cone formation and electrospinnability of a polymer solution could be predicted successfully. The current kinetics of the solutions indicated the morphology of the deposited products. The ball method yielded parameters that indicated whether the polymer solution would be electrospun or electrosprayed:

- Good electrospinning was expected at $l_2 > 8$–10 mm and at $dI/dt_{fb} < 20$%/s.
- Electrospraying together with electrospinning was possible at l_2 values between 0.2 and 8–10 mm and at dI/dt_{fb} values between 20 and 200%/s.
- Electrospinning could not be expected at $l_2 < 0.2$ mm and at $dI/dt_{fb} > 200$%/s.

This range of parameters was determined on the basis of the experiments performed in this study, and it was possible that the range could be corrected. This did not disprove that there was a correlation between the electrospinning and electrospraying and ball-current kinetics parameters and that the proposed method of electrospinning simulation would be suitable for a preliminary testing of the polymer electrospinnability. Although it does not provide detailed information about the electrospun fibers, it could be used to screen for the electrospinnability of polymer solutions.

ACKNOWLEDGMENTS

The authors thank Anthony Bristow for his linguistic revision of the manuscript and Stora Enso Oyj for its financial support of this study.

REFERENCES

1. Ramakrishna, S.; Fujihara, K.; Teo, W.-E.; Lim, T.-C.; Ma, Z. An Introduction to Electrospinning and Nanofibres; World Scientific: Singapore, **2005**.
2. Subbiah, T.; Bhat, G. S.; Tock, R. W.; Pararneswaran, S.; Ramkumar, S. S. *J. Appl. Polym. Sci.* **2005**, *96*, 557.
3. Huang, Z. M.; Zhang, Y. Z.; Kotaki, M.; Ramakrishna, S. *Compos. Sci. Technol.* **2003**, *63*, 2223.
4. Miao, J.; Miyauchi, M.; Simmons, T. J.; Dordick, J. S.; Linhardt, R. J. *J. Nanosci. Nanotechnol.* **2010**, *10*, 5507.
5. Schiffman, J. D.; Schauer, C. L. *Polym. Rev.* **2008**, *48*, 317.
6. Persano, L.; Camposeo, A.; Tekmen, C.; Pisignano, D. *Macromol. Mater. Eng.* **2013**, *298*, 504.
7. Richard-Lacroix Marie, P. C. *Sci. China Chem.* **2013**, *56*, 24.
8. Reneker, D. H.; Yarin, A. L.; Zussman, E.; Xu, H. *Adv. Appl. Mech.* **2007**, *41*, 43.
9. Naebe, M.; Lin, T.; Wang, X. Carbon Nanotube Reinforced Electrospun Polymer Nanofibers; InTech: Rijeka, Croatia, **2010**; p 309.
10. Reneker, D. H.; Yarin, A. L. *Polymer* **2008**, *49*, 2387.
11. Zahedi, P.; Rezaeian, I.; Ranaei-Siadat, S. O.; Jafari, S. H.; Supaphol, P. *Polym. Adv. Technol.* **2010**, *21*, 77.
12. Bayley, G. M.; Mallon, P. E. *Polymer* **2012**, *53*, 5523.
13. Li, J.; Vadahanambi, S.; Kee, C.-D.; Oh, I.-K. *Biomaterials* **2011**, *12*, 2048.
14. Bhardwaj, N.; Kundu, S. C. *Biotechnol. Adv.* **2010**, *28*, 325.
15. Haghi, A. K.; Zaikov, G. Advances in Nanofiber Research; iSmithers Rapra Technology, **2011**.
16. Li, D.; Zhou, X.; Jinglan, Y.; Yu, F.; Wang, X. *J. Appl. Polym. Sci.* **2010**, *117*, 767.
17. Tan, L.; Chen, H.; Pan, D.; Pan, N. *J. Appl. Polym. Sci.* **2008**, *110*, 1997.
18. Hancock, T. A.; Spruiell, J. E.; White, J. L. *J. Appl. Polym. Sci.* **1977**, *21*, 1227.
19. Wendorff, J. H. Electrospin **2010**. January 26th to 29th Melbourne. Program and Abstracts; Melbourne, Australia, Langham, **2010**; p 7.
20. Forward, K. M.; Flores, A.; Rutledge, G. C. *Chem. Eng. Sci.* **2013**, *104*, 250.
21. Fong, H.; Chun, I.; Reneker, D. H. *Polymer* **1999**, *40*, 4585.
22. Liu, H. Q.; Hsieh, Y. L. *J. Polym. Sci. Part B: Polym. Phys.* **2002**, *40*, 2119.
23. Koski, A.; Yim, K.; Shivkumar, S. *Mater. Lett.* **2004**, *58*, 493.
24. Hong, P. D.; Chou, C. M.; He, C. H. *Polymer* **2001**, *42*, 6105.

25. Vetcher, A. A.; Gearheart, R.; Morozov, V. N. *Polym. J.* **2007**, *39*, 878.
26. McKee, M. G.; Hunley, M. T.; Layman, J. M.; Long, T. E. *Macromolecules* **2006**, *39*, 575.
27. McKee, M. G.; Elkins, C. L.; Long, T. E. *Polymer* **2004**, *45*, 8705.
28. Hunley, M. T.; Mckee, M. G.; Long, T. E. *J. Mater. Chem.* **2007**, *17*, 605.
29. Ohkawa, K.; Minato, K.; Kumagai, G.; Hayashi, S.; Yamamoto, H. *Biomacromolecules* **2006**, *7*, 3291.
30. Gupta, P.; Elkins, C.; Long, T. E.; Wilkes, G. L. *Polymer* **2005**, *46*, 4799.
31. Gennes, P. G. Scaling Concepts in Polymer Physics; Cornell University Press: Ithaca, NY, **1979**
32. Shenoy, S. L.; Bates, W. D.; Wnek, G. *Polymer* **2005**, *46*, 8990.
33. Pattamaprom, C.; Hongrojjanawiwat, W.; Koombhongse, P.; Supaphol, P.; Jarusuwannapoo, T.; Rangkupan, R. *Macromol. Mater. Eng.* **2006**, *291*, 840.
34. Uyar, T.; Besenbacher, F. *Polymer* **2008**, *49*, 5336.
35. Kowalczyk, T.; Nowicka, A.; Elbaum, D.; Kowalewski, T. A. *Biomacromolecules* **2008**, *9*, 2087.
36. Zhang, C. X.; Yuan, X. Y.; Wu, L. L.; Han, Y.; Sheng, J. *Eur. Polym. J.* **2005**, *41*, 423.